JOURNAL OF SOLID STATE CHEMISTRY 3, 217–226 (1971)

A Dislocation Model for Two-Level Electron-Hopping Conductivity in V_2O_5: Implications for Catalysis

JEROME H. PERLSTEIN

Department of Chemistry, The Johns Hopkins University, Baltimore, Maryland 21218

Received October 23, 1970

The electrical conductivity of single-crystal V_2O_5 and V_2O_5 doped with copper (α phase) has been measured along the c axis from 77°K to 298°K. Ln σ vs. $1/T$ can be approximated by two straight lines with an average activation energy above 170°K of 0.20 eV and below 170°K of 0.077 eV. Comparison with EPR data and with the V_2O_5-β phase leads to an interpretation for the high-temperature conductivity as arising from thermal excitation of electrons from vanadium-pair traps with an activation energy of 0.15 eV and electron hopping from one vanadium site to another with an activation energy of 0.05 eV. Together with the Seebeck coefficient, the low-temperature data also require direct electron hopping between traps with an activation energy of 0.077 eV. A dislocation model is presented to account for the vanadium pair traps, the electrical conductivity and EPR data. The model require the formation of interstitial oxygen which it is suggested may be involved in the catalytic properties of V_2O_5.

Introduction

The phase studies of Flood, Krog, and Sorum (*1, 2*) have shown that addition of monovalent metals to V_2O_5 produced a series of new phases, $M_xV_2O_5$, each phase being characterized by a range of x. For example, in the case of sodium it has been shown by X-ray analysis that the gross V_2O_5 structure is maintained for $x \leqslant 0.02$, called the α phase (*3, 4*). For larger values of x, a new phase appears called β whose X-ray structure is stable over the range $0.22 \leqslant x \leqslant 0.40$. Other phases with x ranging up to one have been found but studies of their physical properties have been limited. Experimental attention has mainly been centered on the α and β phases.

Extensive studies on the electrical, magnetic, and magnetic resonance properties of the β phase (also called vanadium bronze) have shown that the incorporation of alkali metal into V_2O_5 causes a reduction in valence of the vanadium from V to IV by donation of the alkali metal valence electron to the vanadium sites (*5–7*). Moreover, the reduced valence state of the vanadium is not localized, but moves by way of electron hopping (small polarons) from one vanadium site to another. Such a picture is supported by the absence of a Knight shift in the NMR resonance of Li^7 in $Li_{0.33}V_2O_5$ indicating that the 2s valence electron of Li has been lost to the host structure (*8*); by the magnetic susceptibility of the bronzes which show an effective magnetic moment corresponding to one unpaired electron for each alkali metal atom added (*9*); by electrical conductivity and Hall effect measurements on single crystals which indicate that each electron which contributes to the magnetic susceptibility also contributes to the Hall effect (*10*); by the constant value with temperature change of the Seebeck coefficient indicating a constant number of charge carriers (*9–11*); and by a semiquantitative fit of the data from the above experiments to an energy level diagram for the V^{4+} ion (*10*).

Although the α phase of V_2O_5 ($x \leqslant 0.02$) is orthorhombic (*12, 13*), whereas the β phase structure is monoclinic (*14, 15*), both structures have similar distorted VO_6 octahedra with similar V–O bond distances (*16*) and a near neighbor vanadium–vanadium distance which repeats itself along the high conductivity axis of the two phases. In $Na_{0.33}V_2O_5$ the closest V–V distance is 3.07 Å; the closest repeating V–V distance in the α phase is 3.08 Å. It would, therefore, be expected that the α phase should show electron hopping transport like the β phase.

The electrical conductivity of V_2O_5 has been measured numerous times (*17–26*). The results together with Seebeck effect data and magnetic resonance data have been interpreted as indicating the presence of V(IV) with electron hopping from site to site (*26–30*). Nevertheless, there are a number of disturbing features of this model. The activation for conduction in V_2O_5 is about 0.2 eV (obtained from $\sigma = \sigma_0 e^{-\Delta E/kT}$), whereas in the β phase it is only 0.05 eV. If an electron hops from one vanadium site to a near neighbor in both α and β phases, then the activation energies should be similar. The Seebeck coefficient for V_2O_5 is negative at all temperatures indicating negative charge carriers, but the absolute value of the Seebeck coefficient shows a maximum (*18, 24, 26*). Simple electron-hopping transport should give a constant Seebeck coefficient over a wide temperature range as is exhibited by the β phase. The magnetic susceptibility of V_2O_5 is temperature independent and quite large equal to 100×10^{-6} emu/mole (*31*). The origin of this is unknown.

The present work was initiated to try and understand the differences as well as the similarities between the α and β phases and hopefully to shed some light on the bulk properties of V_2O_5 which make it such a useful oxidation catalyst. In this regard, it has been stated that V_2O_5 catalytic oxidation changes the catalyst into a reduced oxide phase V_6O_{13} (*32, 33*), which is a member of the homologous series V_nO_{2n+1}. V_3O_7 is another member of this series which has been positively identified (*34, 35*). A dislocation mechanism for the formation of these reduced phases from the V_2O_5 parent has been proposed by Andersson and Hyde and by Gillis, in which ordering of anion vacancies results in shear planes along whose boundaries are present the microdomains of the lower oxide (*36, 37*). There appears to be some disagreement, however, as to the importance of the dislocation mechanism for formation of these lower oxides (*38, 39*).

We wish to show that the electrical properties of V_2O_5 can be best understood as arising from the formation of dislocations and that there are at least two energy levels within the shear structures in which electron-hopping transport occurs with electrons thermally activated from one level to another.

Experimental

Single crystals of V_2O_5 and V_2O_5 doped with copper were grown by slow cooling of the melt. Approximately 80 g of V_2O_5 powder of 99.94% purity (impurities as reported by Vanadium Corporation of America were $SiO_2 = 0.02\%$, $Cl = 0.005\%$, $Fe_2O_3 = 0.015\%$) were placed in a platinum dish heated to 750°C in air and held at this temperature for 16 hr in a Dyna kiln. Slow cooling through the melting point was achieved manually at a rate of 10°C/hr. Samples were cooled down to approximately 600°C and then allowed to cool to room temperature under the thermal mass of the kiln. For samples containing copper, Fisher purified copper dust was mixed into the V_2O_5 before heating. Composition is reported based on the total copper added.

Single crystals for electrical conductivity measurements were cleaved with a razor blade from the cooled V_2O_5 mass. Crystals grew elongated along the *c* axis and were easily cleaved perpendicular to the *b* axis (V_2O_5 crystallizes with an orthorhombic unit cell, space group *Pmnm* with $a = 11.51$, $b = 4.37$, and $c = 3.56$. The *b* and *c* axis are often interchanged). Typical sample dimensions for conductivity measurements were $2 \times 1 \times 0.03$ mm^3.

Electrical Conductivity

Electrical conductivity was measured using a four-probe technique, using two current leads and two potential leads painted directly onto the crystal to eliminate contact resistance. The crystal was mounted on a crystal holder to be described elsewhere. Electrical leads were painted on the crystal using DuPont silver conducting paste, no. 4929. On one sample a grounded guard ring was painted around the entire crystal near a current lead but was found to have no effect on the electrical conductivity either at room temperature or at 77°K. The crystal holder was placed in a variable temperature cryostat and pumped down to approximately 1μ of He. No noticeable changes were observed in the electrical conductivity even after continuous pumping for several days at room temperature. Nor were there any noticeable changes in the conductivity after passing 0.4 mA through sample no. 57 (see Table I) of dimensions $1.6 \times 0.5 \times 0.03$ mm for 8 days under 1-μ helium pressure indicating the electrical conductivity at room temperature has no ionic component.

Current for the samples was supplied by a 1.35-V mercury cell and was determined by measuring the potential across a standard resistor in series with the sample using a battery operated Keithley electrometer no. 200B with 10^{14} Ω input impedance. (Standard resistors of 10^6–10^{11} Ω available from Keithley Corporation, 2% precision.) Potential across the crystal was measured with another

Keithley no. 200B electrometer. Thermal emf's were eliminated by measuring the potential with forward and reverse current. Resistances were independent of the measuring current which was varied over several orders of magnitude. Sample dimensions for calculating the conductivity, σ, were measured using a calibrated-microscope eyepiece.

Temperature of the samples was measured with a platinum resistance thermometer mounted near the crystal. The thermometer was calibrated at the ice point and boiling points of water and checked for accuracy at the sublimation point of vigorously heated CO_2, and the boiling points of O_2 and N_2. Temperatures were accurate to within a few tenths of a degree. Electrical conductivity was measured both cooling and heating the samples over the same temperature interval. No hysteresis in σ was observed.

Results and Discussion

I. Electrical Properties for $T > 170°K$

Table I and Figs. 1 and 2 show the results of the electrical conductivity measurements along the c axis for "pure" V_2O_5 and V_2O_5 doped with various amounts of copper. From the data in the table, it can be seen that the addition of 0.4-mole % copper increases the room temperature conductivity of V_2O_5 by one order of magnitude. Patrina and Ioffe (*24*) have shown that prolonged heating of single crystals of V_2O_5 in a stream of oxygen at 580 to 600°C had little effect on the room temperature electrical conductivity of "pure" V_2O_5. Volzhenskii and Pashkovskii (*26*) find similar results along the

TABLE I

ACTIVATION ENERGIES AND ROOM-TEMPERATURE CONDUCTIVITIES ALONG THE C AXIS FOR V_2O_5 DOPED WITH COPPER

Sample no.	Composition	ΔE(eV) ($T > 170°K$)	ΔE(eV) ($T < 170°K$)	$\sigma(\Omega^{-1}\,cm^{-1})$ ($T = 298°K$)
59	V_2O_5	0.170	—[a]	8.3×10^{-4}
60	V_2O_5	0.189	0.0781	8.8×10^{-4}
48	$Cu_{0.0043}V_2O_5$	0.193	0.0758	8.6×10^{-3}
49	$Cu_{0.0043}V_2O_5$	0.208	0.0752	8.4×10^{-3}
52	$Cu_{0.0062}V_2O_5$	0.235	—[b]	9.1×10^{-3}
54	$Cu_{0.0083}V_2O_5$	0.222	0.0759	14.4×10^{-3}
57	$Cu_{0.02}V_2O_5$	0.237	0.0790	12.9×10^{-3}

[a] Sample resistance too high to measure.

[b] Poor contacts—erratic behavior.

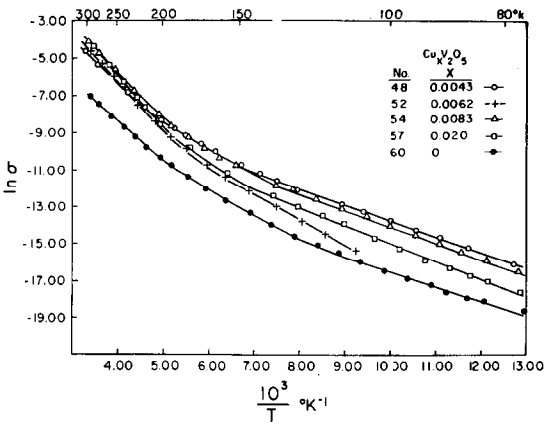

FIG. 1. Natural logarithm of σ along the c axis vs. $10^3/T$ for single-crystal V_2O_5 and V_2O_5 doped with copper grown in air.

c axis for samples grown under 5 atm of oxygen. It would thus appear that the room-temperature behavior of V_2O_5 is dominated by the presence of impurities. The addition of copper increases the impurity content and thus increases the electrical conductivity.

Perlstein and Sienko (*10*) have shown from electrical conductivity, Seebeck effect and Hall effect measurements, that in the β phase of V_2O_5, specifically for $Na_{0.33}V_2O_5$, the room-temperature electrical properties are due to mobility-activated electrons (small polarons) hopping between neighboring vanadium sites. The mobility has an activation energy of about 0.05 eV and a value of 0.2 $cm^2/Vsec$ at room temperature. Considering the similarities in the local vanadium site symmetry between the α and β phases, it seems reasonable to

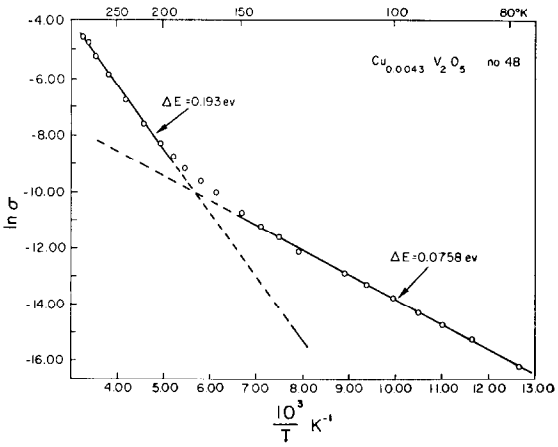

FIG. 2. Natural logarithm of σ along the c axis vs. $10^3/T$ for sample no. 48. Data are approximated by two straight lines with activation energies based on the equation $\sigma = \sigma_0 e^{-\Delta E/kT}$.

assume that the room-temperature mobility and its activation energy for the α phase should be similar to that found for the β phase. Under such an assumption, we can calculate the density of charge carriers in any of our samples from the value of σ and the assumed value of 0.2 cm^2/Vsec for the mobility, μ. For $Cu_{0.0043}V_2O_5$ (sample no. 48),

$$n = \frac{\sigma}{e\mu} = \frac{8.6 \times 10^{-3}}{(1.6 \times 10^{-19})(0.2)} = 2.7 \times 10^{17}/\text{cm}^3 \quad (1)$$

There have been several reports on the measurement of the Hall effect in V_2O_5 with resulting mobilities of 0.03 to 2.2 cm^2/Vsec (*30*, *41–43*). The results are usually reported for compressed samples although Ioffe and Patrina (*30*) claimed to have measured a room temperature mobility of 0.03 cm^2/Vsec along the *c* axis for one crystal. No details were given. Their Hall coefficient was 20 cm^{-3}/C which corresponds to 3.1×10^{17} electrons/cm^3 (assuming $R = 1/ne$ for the hopping process. This has been justified for the β phase (*55*) in terms of the Friedman and Holstein small polaron mobility (*44*)).

Ragle (*40*) has shown that addition of copper to V_2O_5 produces two-overlapping 15-line EPR spectra for $H \| b$ at 77°K. He interpreted this to mean that the electron from each added copper is delocalized over a pair of vanadium sites, each site having a nuclear spin of 7/2. The pair of sites would thus have a nuclear spin $I = 7$ and thus produce $2I + 1$ or 15 lines. The intensity of the lines found by Ragle was in agreement with that predicted by such a model. The fact that there were two sets of lines was interpreted to mean the presence of two slightly different environments for the V–V pairs.

The density of charge carriers calculated from Eq. (1) is considerably less than the density of copper atoms added which for sample no. 48 is 4.8×10^{19}/cm^3. (Based on a molecular weight of 182 and a density of 3.36 g/cm^3 for V_2O_5.) If our estimate of the mobility is correct, then the carriers responsible for the conductivity calculated in Eq. (1) must first be thermally activated from a donor level or trapping site. As a model for such a trapping level, we consider the V–V pair formation found by Ragle. The molecular orbital formed by such a pair will have an energy lower than a single vanadium site. Figure 3 shows an energy level scheme for the vanadium pair trapping levels and the conduction level. The density of trapping sites, N_t, is assumed equal to one-fourth the density of conduction sites, N_c. (This will be justified later.) From Table I it can be seen that the average activation energy for conduction for $T > 170$°K is 0.20 eV (based on

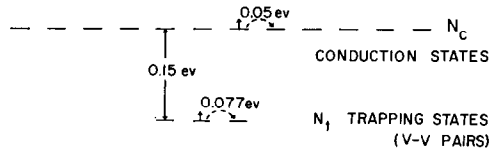

FIG. 3. Conduction model for V_2O_5 showing vanadium pair trapping states of density N_t occurring 0.15 eV below single vanadium site conducting state of density $N_c = 4N_t$. Hopping occurs in both levels with mobility activation energy shown.

the equation $\sigma = \sigma_0 e^{-\Delta E/kT}$). This activation energy consists of two parts: (a) thermal activation of electrons from the vanadium pair trapping levels into the conduction levels, and (b) mobility activation from one conduction state to another. If the mobility has an activation energy of 0.05 eV as in the β phase, then thermal excitation of carriers from the traps must require an activation energy of 0.20–0.05 = 0.15 eV. This is also indicated in Fig. 3. We can now calculate the density of carriers in the conduction states from this model. If the density of electrons in the conduction states is n_c and the density in the trapping states is n_t, then application of Boltzmann statistics gives

$$\frac{n_c}{n_t} = \frac{N_c e^{-E_c/kT}}{N_t e^{-E_t/kT}}.$$

With $\Delta E = E_c - E_t = 0.15$ eV $\gg kT$, then $n_t \approx$ [Cu]

$$\therefore \quad n_c = \frac{[\text{Cu}]\, N_c}{N_t} e^{-\Delta E/kT}, \quad (2)$$

$N_c \approx 4N_t$ and [Cu] $= 4.8 \times 10^{19}$/cm^3 for sample no. 48,

$$\therefore \quad n_c = 6.0 \times 10^{17}/\text{cm}^3 \text{ at } T = 298°\text{K}.$$

This is in fair agreement with the density of carriers calculated from the electrical conductivity and an assumed mobility of 0.2 cm^2/Vsec as observed in the β phase. On this basis the model of Fig. 3 is reasonable.

II. Electrical Properties for $T < 170$°K

Below $T = 170$°K, Figs. 1 and 2 and Table I show that the natural logarithm of the electrical conductivity vs. temperature has an activation energy of about 0.077 eV which is less than for $T > 170$°K. Several salient features should be pointed out about this low temperature behavior:

(a) Samples doped with copper have a higher conductivity at low temperatures than do "pure" V_2O_5 samples. The presence of copper impurity thus

appears to contribute to both the low temperature and high-temperature electrical properties.

(b) The activation energy at low temperature shows no trend with copper concentration. The values are approximately the same in the doped samples as in "pure" V_2O_5 even though the doped samples have a conductivity some 10 to 50 times higher than "pure" V_2O_5. We interpret this to mean that hopping does not simply occur between states localized around the copper impurity since this would require the activation energy to decrease as these states become closer together, viz. with increasing impurity content. Such a model has been proposed for the β phase (*7, 45*). However, it is based on activation energies obtained from compressed samples.

(c) As can be seen from Fig. 1, the variation in conductivity at low temperatures from one copper-doped sample to another is not very regular. Some of the samples with low copper content have higher conductivities than some of the samples with higher copper concentration. This would appear to indicate that there is some other contribution to the conductivity along the c axis at low temperatures other than the simple addition of copper. Ioffe and Patrina (*24*) have shown that the low-temperature conductivity can be reduced by annealing samples under oxygen, although as already indicated this has no effect on the room-temperature electrical properties. This indicates to us that the low-temperature conductivity is in part determined by the presence of oxygen defects which is variable from sample to sample. We will not pursue the contribution of the oxygen defect to the conductivity in this paper since it only complicates the basic model which we wish to propose. The low-temperature conductivity is for the most part still governed by the presence of copper.

The simplest model to consider for the low-temperature conductivity is to assume that the electrons in the traps at energy E_t indicated in Fig. 3 can hop from one trap site to another with an activation energy of 0.077 eV. This hopping is feasible if the trap density N_t is much higher than the number of available electrons which we assume for now equal to the copper concentration. We will show shortly that the trap site density is about $5 \times 10^{21}/\text{cm}^3$. Since the low-temperature activation energy for hopping is greater than the high-temperature activation (0.05 eV), the low-temperature mobility of electrons in the trapping states will be less than those electrons which are thermally excited from E_t to E_c. For $T > 170°\text{K}$ the higher mobility will dominate the conductivity.

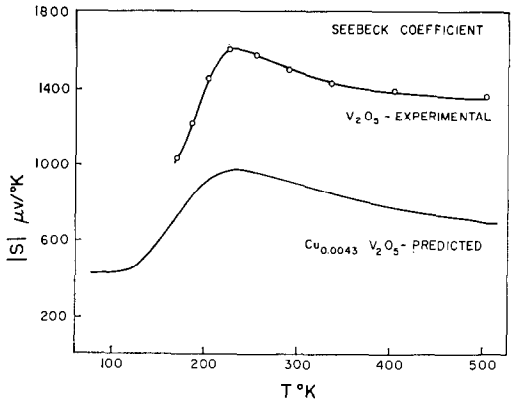

FIG. 4. Absolute value of the Seebeck coefficient vs. temperature. Upper curve is the experimental data of Patrina and Ioffe (24) for a V_2O_5 single crystal. Lower curve is that predicted for sample no. 48 based on Eq. (15) in text.

III. The Seebeck Coefficient

To justify the proposed two energy level hopping mechanism of Fig. 3 we appeal to the Seebeck Coefficient data (*18, 19, 24, 26, 41*). This is found to be negative indicating that the majority carriers are electrons. However, there is also a maximum found in the absolute value of the Seebeck coefficient in the range 250–280°K. The absolute value of the Seebeck coefficient vs. T for one sample of Patrina and Ioffe (*24*) is shown in Fig. 4. Such maxima are indicative of two contributions to the Seebeck effect. Although a maximum would be observed if both electrons and holes were contributing to the electrical conductivity, evidence for hole transport in V_2O_5 is substantially lacking. [Krch (*41*) reports a positive Hall coefficient for $T > 241°\text{K}$ but this has never been verified.] A negative Seebeck effect has always been reported with no indication of a transition to positive values.

If the charge carriers are therefore electrons, it is difficult to see how a maximum in the Seebeck effect could occur if there is only one conduction level. The presence of two conduction levels, however, with different mobilities does yield a maximum in the absolute value of the Seebeck coefficient as we now wish to show.

For a two level conducting system like that in Fig. 3, the Seebeck coefficient is a weighted sum of the Seebeck coefficients for each level (*46*),

$$S = \frac{\sigma_c}{\sigma} S_c + \frac{\sigma_t}{\sigma} S_t, \tag{3}$$

where σ_c and σ_t are the electrical conductivities contributed by electrons in energy level E_c and E_t, respectively and $\sigma = \sigma_c + \sigma_t$. S_c and S_t are the

Seebeck coefficients with respect to each of the conductivity levels,

$$S_c = \frac{k}{e}\left(\frac{\mu_c}{kT} + A_c\right), \tag{4}$$

$$S_t = \frac{k}{e}\left(\frac{\mu_t}{kT} + A_t\right). \tag{5}$$

μ_c and μ_t are the chemical potentials taken with respect to E_c and E_t as the reference points, respectively. In what follows we will assume the kinetic energy transport terms A_c and A_t are both zero for a hopping model. Then

$$\mu_c = E_F - E_c, \tag{6}$$

$$\mu_t = E_F - E_t, \tag{7}$$

where E_F is the Fermi level. (In a one level system E_F would simply be the chemical potential since the reference point can be set arbitrarily equal to zero. We cannot do this in a two-level system). Combining Eq. (6) and (7) we find

$$\mu_t = \mu_c + E_c - E_t = \mu_c + \Delta E.$$

Substituting this for μ_t in Eq. (5) and then combining Eqs. (4) and (5) into (3) gives for the total Seebeck coefficient of the two levels

$$S = \frac{k}{e}\left(\frac{\mu_c}{kT}\right) + \frac{k}{e}\frac{\sigma_t}{\sigma}\left(\frac{\Delta E}{kT}\right). \tag{8}$$

In this expression ΔE is 0.15 eV and the ratio σ_t/σ can be found from graphs like Fig. 2. We still need an expression for the chemical potential, μ_c.

Applying Fermi–Dirac statistics to the two-level model, the density of electrons in the upper conducting level, n_c, is simply

$$n_c = \frac{N_c}{e^{(E_c - E_F)/kT} + 1}. \tag{9}$$

The density of electrons in the lower conducting level is

$$n_t = \frac{N_t}{e^{(E_t - E_F)/kT} + 1}. \tag{10}$$

If all the electrons for conduction in the two levels come from the added copper, then

$$n_c + n_t = [\mathrm{Cu}]$$

or

$$n_c + \frac{N_t}{e^{(E_t - E_F)/kT} + 1} = [\mathrm{Cu}]. \tag{11}$$

For low copper densities, the trapping level (viz., the lower conducting level) will only be partially filled and the Fermi level will thus lie near E_t. Thus $E_c - E_f \gg kT$ which gives an approximation for n_c in Eq. (9)

$$n_c \approx N_c e^{(E_F - E_c)/kT}$$

or

$$\frac{E_F}{kT} = \frac{E_c}{kT} + \ln\frac{n_c}{N_c}. \tag{12}$$

Substituting Eq. (12) for E_F into Eq. (11) and rearranging gives

$$\frac{n_c + N_t - [\mathrm{Cu}]}{N_c\left(\dfrac{[\mathrm{Cu}]}{n_c} - 1\right)} = e^{(E_t - E_c)/kT} = e^{-\Delta E/kT}. \tag{13}$$

In the expression on the left-hand side, $n_c \approx 10^{17}/\mathrm{cm}^3$ at room temperature, $N_t \approx 10^{21}/\mathrm{cm}^3$ and $[\mathrm{Cu}] \approx 10^{19}/\mathrm{cm}^3$. In the numerator we can thus neglect n_c and [Cu] compared to N_t. In the denominator

$$\frac{[\mathrm{Cu}]}{n_c} \approx \frac{10^{19}}{10^{17}}$$

at room temperature so we can drop the -1.

We thus get from Eq. (13)

$$n_c = \frac{N_c[\mathrm{Cu}]}{N_t} e^{-\Delta E/kT}, \tag{14}$$

which is simply the Boltzmann distribution which we used earlier, Eq. (2), to calculate n_c. Substituting Eq. (14) into Eq. (12) and then (12) into (6) gives for the chemical potential, μ_c

$$\frac{\mu_c}{kT} = -\frac{\Delta E}{kT} + \ln\frac{[\mathrm{Cu}]}{N_t}$$

Substituting for μ_c in Eq. (8) gives for the total Seebeck coefficient

$$S = \frac{k}{e}\left(\frac{-\Delta E}{kT} + \ln\frac{[\mathrm{Cu}]}{N_t}\right) + \frac{k}{e}\frac{\sigma_t}{\sigma}\left(\frac{\Delta E}{kT}\right)$$

or

$$S = -\frac{k}{e}\left[\frac{\Delta E}{kT}\left(1 - \frac{\sigma_t}{\sigma}\right) + \ln\frac{N_t}{[\mathrm{Cu}]}\right]. \tag{15}$$

Figure 4 also shows a plot of the absolute value of S vs. T for Eq. (15) with $\Delta E = 0.15$ eV, σ_t/σ determined from Fig. 2, $[\mathrm{Cu}] = 4.8 \times 10^{19}/\mathrm{cm}^3$ and $N_t = 5.7 \times 10^{21}/\mathrm{cm}^3$. We only wish to make a qualitative comparison between the theoretical and experimental curves since Patrina and Ioffe did not intentionally dope their crystals. The shape of the curves is similar with a maximum in the theoretical curve occurring at the appropriate place. Our calculations predict that if the Seebeck effect measurement is extended to lower temperatures, it should flatten out as indicated. The shape of the

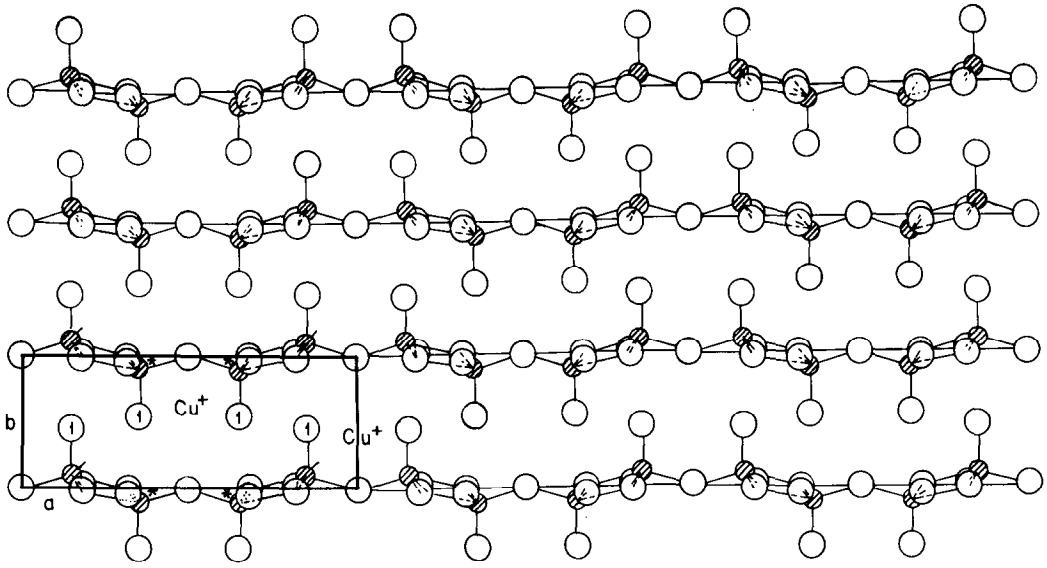

FIG. 5. V_2O_5 structure projected along (001), after Byström, Wilhelmi, and Brotzen (12); $a = 11.51$ Å and $b = 4.37$ Å of unit cell is outlined. Shaded circles are vanadium. Inferred positions of monovalent impurities are shown (3). Preferred cleavage plane is perpendicular to the b axis.

whole curve can be understood as follows: At low temperatures, $\sigma_t/\sigma = 1$ so that the only contribution to the Seebeck effect is from the ln term. At about 170°K, σ_t/σ begins to go much less than one as Fig. 2 indicates so that the first term of Eq. (15) begins to contribute to S causing a large increase in $|S|$. At still higher temperatures $\sigma_t/\sigma \to 0$ so that only $\Delta E/kT$ governs the change in the Seebeck coefficient. The absolute value of this term decreases with increasing T thus producing the maximum.

Dislocation Model for the Conduction Levels

In this section we would like to introduce a model for the conduction levels in V_2O_5 based in part on the X-ray crystallographic structure of Byström et al. (*12*) and Bachmann et al. (*13*).

Figure 5 is a projection of the V_2O_5 structure onto (001). Vanadium atoms labeled by a prime ⊜′ are in the a–b plane ($z = 0$). Those labeled by a star ⊜* are off the a–b plane at $z = c/2$. The V′–V* distance is 3.08 Å. The (010) planes are held together by weak V–O_1–V bonds with one V–O_1 distance of 2.81 Å. Breaking of this weak bond accounts for the preferred cleavage of the V_2O_5 crystals perpendicular to the b axis. Figure 5 also shows the position of monovalent impurity atoms as inferred from the structure by Hardy et al. (3). There are two possible equivalent positions for the copper at (0, 0.397, 1/2) and (1/2, −0.397, 0). Figure 6 shows the V_2O_5 structure projected onto (010). The short 3.08 Å V′–V* distance zig-zagging along the c axis is more clearly indicated. We postulate that hopping from V′ to V* to V′, etc. occurs along the c axis with an activation energy of 0.05 eV similar to the hopping transport in the β phase where the V–V distance is 3.07 Å. However, this does not account for the additional thermal activation of 0.15 eV from a V–V trapping center. As has been already indicated, EPR studies at 77°K on single crystals doped with copper show the formation of vanadium pair centers with an electron delocalized over two vanadium sites. In a study of the EPR spectra of zone refined V_2O_5 crystals as a function of rotation about the a

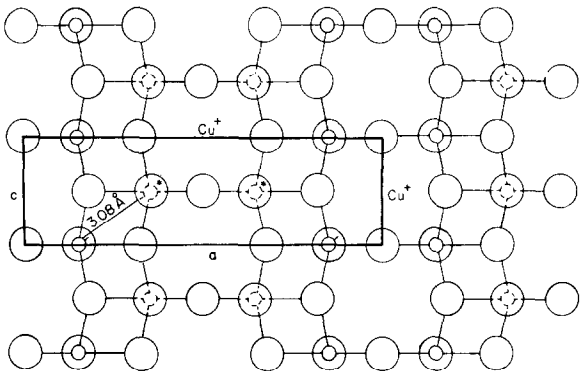

FIG. 6. V_2O_5 structure projected along (010) drawn after Gillis and Boesman (47); $a = 11.51$ Å and $c = 3.56$ Å outlined. Small circles are vanadium with dotted ones below a–c plane and solid ones above. Zig-zagging of vanadiums separated by 3.08 Å along c axis is clearly seen.

and c axis, Gillis and Boesman (*47*) concluded that one possibility for the formation of a vanadium pair center was the presence of oxygen defects, specifically the presence of O_1 defects. This would allow for overlap of two vanadium wavefunctions along the b axis. Each O_1 defect, however, leaves behind two electrons in the structure. Since no 8-line EPR spectra was observed, they concluded that the other electron from the O_1 defect participated in V(III) formation with another electron from some other O_1 defect. No EPR spectrum of V(III) would be seen because of the large zero-field splitting for this species.

It seems unlikely to us that V(III) could be stabilized in a V(V) lattice. The large coulomb repulsion between electrons on V(III) would favor the formation of V(IV). We, therefore, wish to introduce another mechanism for the formation of the vanadium pair site which is consistent with the EPR spectrum as well as the electrical properties described above.

Since cleavage perpendicular to the b axis is so easy, we can consider the formation of a dislocation in the V_2O_5 structure by slippage of a–c planes as illustrated in Fig. 7. One a–c plane has slipped 0.2 lattice spacings along the a axis and 0.5 lattice spacings along the c axis. Evidence of dislocation lines which could be produced by this mechanism have been observed in electron micrographs of V_2O_5 (*38*). The production of such a dislocation requires the formation of one oxygen interstitial/unit cell as indicated by O_i. The nature of such an interstitial is not known, but it could conceivably exchange with oxygen in the gas phase and be involved in catalytic oxidation. ^{18}O exchange studies indicate that atomic oxygen from the V_2O_5 catalyst is involved in one mechanism of exchange (*48*). Molecular oxygen from V_2O_5 has also been proposed as a possible exchange species (*48–52*). Even if every a–c plane in the V_2O_5 structure were to be involved in the formation of a dislocation, this would amount to the production of one interstitial oxygen per V_4O_{10} unit cell or 10% of the total oxygen. V_2O_5 prepared from oxygen enriched with ^{18}O shows less than 10% exchange with gaseous oxygen (*53, 54*). Thus, if V_2O_5 oxygen is involved in exchange, it appears to be small and may involve the O_i interstitial formulated above. If the oxygen interstitial is present as a charged species, then ionic conductivity should be manifest at temperatures well above room temperature. Reduction of V_2O_5 should also occur preferentially perpendicular to the a–b or a–c planes by migration of interstitial oxygen along the tunnels parallel to the c or b axis.

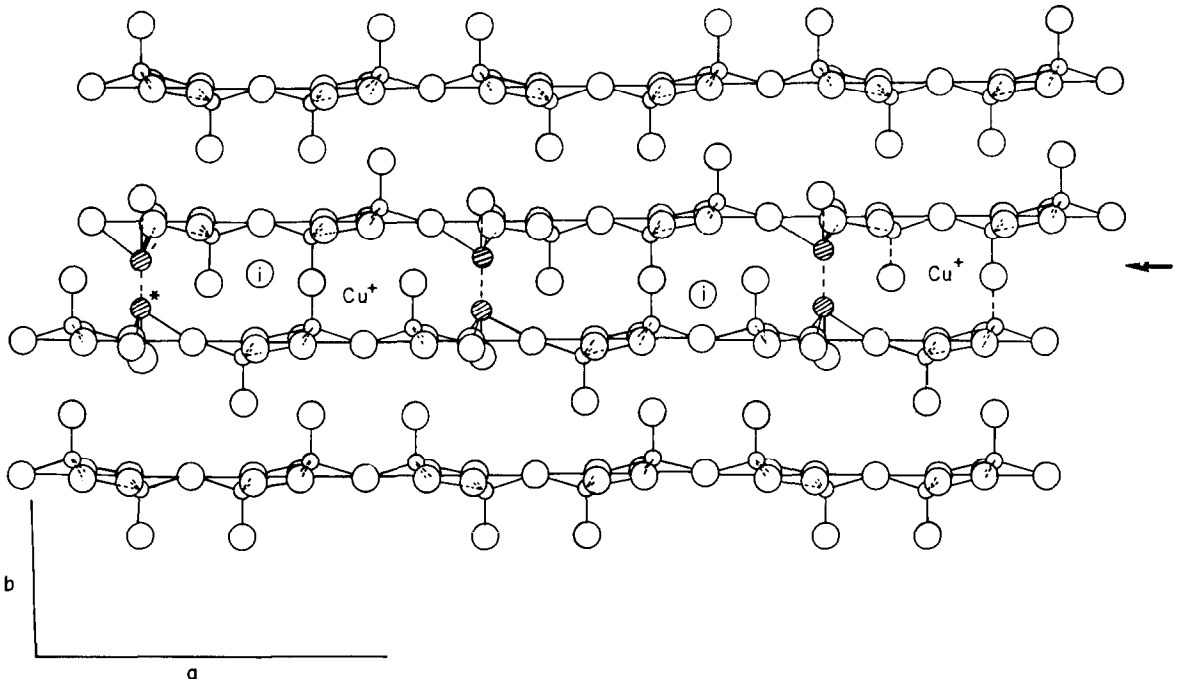

FIG. 7. Proposed dislocation structure for V_2O_5. Dislocation occurs at arrow perpendicular to b producing one V^I–V^* pair/V_2O_5 unit cell along the slip as indicated by shaded circles and one oxygen interstitial, ⓘ. Possible positions for the interstitial oxygen and Cu^+ are indicated.

Figure 7 also indicates that the dislocation brings two vanadium sites in different planes into coincidence along the *b* axis. This occurs all along the dislocation and allows the formation of one vanadium pair/unit cell along the slip plane. Electrons from monovalent interstitial impurities such as copper or both electrons from an O_i interstitial which has left the lattice can form the EPR centers observed by Ragle and by Gillis and Boesman. The overlapping of two 15-line spectra observed by Ragle may be due to the slight difference in energy of those V–V pairs which have interstitial oxygen vacancies as neighbors as opposed to copper ions as neighbors along the dislocation.

Looking along the *c* axis in the slip plane, every unit cell contains one such V–V pair. The pairs are separated by 3.55 Å along the *c* axis and thus should require a larger activation energy for electron hopping than between single vanadium centers which are closer together (3.08 Å). We postulate the low-temperature ($T < 170°K$) electrical conductivity to be due to hopping between these pair states with an activation energy of 0.077 eV. At higher temperatures, thermal activation of carriers from this trapping level is equivalent to breaking the molecular orbital forming the V–V pair with the electron left on a single vanadium site. We postulate that this requires an activation energy of 0.15 eV. The electron then hops between single vanadium sites which form a zig-zag chain along the *c* axis. The activation for this process is 0.05 eV.

As can be deduced from Fig. 7, along the dislocation there are four times as many single vanadium sites (including the single sites belonging to a pair) as there are V–V trapping centers (Vanadium atoms that don't form traps or are not nearest neighbors to a trap are not counted). The density of trapping centers associated with the dislocations is easily computed from the unit cell dimensions and unit cell volume of V_2O_5. Each unit cell along the dislocation contains one V–V trapping center. The unit cell volume is $177 \times 10^{-24}/cm^3$. Thus, the density of trapping centers, N_t, is

$$\frac{1}{177 \times 10^{-24}} = 5.7 \times 10^{21}/cm^3.$$

Ragle (*40*) also found that for copper concentrations greater than 0.78 mole %, a second narrow structureless line appeared in the EPR spectrum superimposed upon the hyperfine spectrum. Gillis and Boesman (*47*) found a similar narrow line for V_2O_5 samples treated in a vacuum of 10^{-7} mm at 160°C over a period of 2 months or treated over a period of 3 weeks at 300°C. Ragle interpreted the narrow line as due to a mobile electron. Based on our model of Fig. 3, the electrons in the trapping states must yield a 15-line spectrum. This requires the hopping frequency among these states to be less than the spin-lattice relaxation frequency implying that the electron is localized long enough for the EPR hyperfine structure to be observed. Thermal excitation of electrons from E_t to E_c could produce the narrow line observed by Ragle since the mobility of electrons in these states is higher than in the trapping states. However, at 77°K (the temperature at which the hyperfine spectrum appears) the density of electrons in E_c as calculated from Eq. (2) for a copper concentration of 0.78 mole % is only 4.4×10^{10} electrons/cm^3 which is too small to have been observed by EPR. A second possibility for the narrow line is based on the proposed dislocation model of Fig. 7 and in part suggested by Gillis and Boesman. Segregation of either copper or O_i vacancies along the dislocation should produce a sufficient density of V–V pairs so that exchange interaction between such pairs becomes important. The single line can then be interpreted as due to exchange narrowing.

Conclusions

The presence of point defects in the form of anion vacancies or impurity interstitials is not sufficient to account for the electrical properties of V_2O_5. If most of the vanadium sites are involved in hopping transport, their high density ($\sim 10^{22}/cm^3$) relative to the point defect density ($\sim 10^{19}$) would result in all defect sites being empty at room temperature and, thus, all electrons from the defect sites would be participating in hopping transport. The experimental evidence indicates that, in fact, most of the electrons are still trapped out at room temperature. This requires the presence of a density of states for trapping centers which is comparable with the single vanadium site density.

The change in activation energy as a function of copper concentration is not what would be expected for a model in which hopping occurs between states localized around impurity centers. Such a model predicts an activation energy which decreases with increasing copper concentration. If anything, the trend in activation energies is increasing with increasing copper concentration.

The proposed dislocation model accounts naturally for the high trap site density, the EPR spectrum and the observed maximum in the temperature dependence of the absolute value of the Seebeck coefficient.

The model predicts the presence of interstitial oxygen which, if present as a charged species, should be highly mobile at high temperature and manifest itself in the form of ionic conductivity. The presence of such mobile interstitial oxygen may be responsible for the properties of V_2O_5 as an oxidation catalyst.

Acknowledgment

Acknowledgment is made to the Research Corporation and to the donors of the Petroleum Research Fund administered by the American Chemical Society for support of this research.

References

1. H. Flood and H. Sorum, *Tidsskr. Kjemi Bergv. Met.* **5**, 55 (1943).
2. H. Flood, Th. Krog, and H. Sorum, *Tidsskr. Kjemi Bergv. Met.* **3**, 32 (1946); **5**, 59 (1946).
3. A. Hardy, J. Galy, A. Casalot, and M. Pouchard, *Bull. Soc. Chim. Fr.*, 1056 (1965).
4. P. Hagenmüller, J. Galy, M. Pouchard, and A. Casalot, *Mater. Res. Bull.* **1**, 45 (1966).
5. M. J. Sienko, *Advan. Chem. Ser.* No. 39 (1963).
6. M. Pouchard, A. Casalot, G. Villeneuve, and P. Hagenmüller, *Mater. Res. Bull.* **2**, 877 (1967).
7. A. Casalot and P. Hagenmüller, *J. Phys. Chem. Solids* **30**, 1341 (1969).
8. J. Gendell, R. M. Cotts, and M. J. Sienko, *J. Chem. Phys.* **37**, 220 (1962).
9. M. J. Sienko and J. B. Sohn, *J. Chem. Phys.* **44**, 1369 (1966).
10. J. H. Perlstein and M. J. Sienko, *J. Chem. Phys.* **48**, 174 (1968).
11. Z. I. Ornatskaya, *Sov. Phys.-Solid State* **6**, 978 (1964).
12. A. Byström, K. A. Wilhelmi, and O. Brotzen, *Acta Chem. Scand.* **4**, 1119 (1950).
13. H. G. Bachmann, F. R. Ahmed, and W. H. Barnes, *Z. Krist.* **115**, 110 (1961).
14. A. D. Wadsley, *Acta Crystallogr.* **8**, 695 (1955).
15. R. P. Ozerov, G. A. Gol'der, and G. S. Zhdanov, *Sov. Phys.-Crystallogr.* **2**, 211 (1957).
16. H. G. Bachmann and W. H. Barnes, *Z. Krist.* **115**, 215 (1961).
17. A. N. Arsen'eva and B. V. Kurchatov, *Zh. Eksp. Teor. Fiz.* **4**, 576 (1934).
18. B. M. Hokhberg, *Zh. Eksp. Teor. Fiz.* **7**, 1090 (1937).
19. B. M. Hokhberg and M. S. Sominski, *Zh. Eksp. Teor. Fiz.* **7**, 1099 (1937).
20. J. Boros, *Z. Phys.* **126**, 721 (1949).
21. V. A. Yurkov, *Zh. Eksp. Teor. Fiz.* **22**, 223 (1952).
22. S. Kachi, T. Takada, and K. Kosuge, *J. Phys. Soc. Jap.* **18**, 1839 (1963).
23. J. Haemers, *C. R. H. Acad. Sci.* **259**, 3740 (1964).
24. I. B. Patrina, V. A. Ioffe, *Sov. Phys.-Solid State* **6**, 2581 (1965).
25. T. Allersma, R. Hakim, T. N. Kennedy, and J. D. Mackenzie, *J. Chem. Phys.* **46**, 154 (1967).
26. D. S. Volzhenskii and M. V. Pashkovskii, *Sov. Phys.-Solid State* **11**, 950 (1969).
27. V. A. Ioffe and I. B. Patrina, *Sov. Phys.-Solid State* **6**, 2425 (1965).
28. L. V. Dmitrieva, V. A. Ioffe, and I. B. Patrina, *Sov. Phys.-Solid State* 7, 2228 (1966).
29. V. A. Ioffe and I. B. Patr,na, *Sov. Phys.-Solid State* **10**, 639 (1968).
30. V. A. Ioffe and I. B. Patrina, *Phys. Status Solidi* **40**, 389 (1970).
31. J. B. Sohn, Ph.D. Thesis, Cornell University, 1965.
32. G. L. Simard, J. F. Steger, R. J. Arnott, and L. A. Siegel, *Ind. Eng. Chem.* **47**, 1424 (1955).
33. V. Y. Volfson, Y. V. Zhigailo, E. F. Totskaya, and V. V. Raksha, *Kinet. Catal. (USSR)* **6**, 138 (1965).
34. D. Thomas, J. Tudo, and G. Tridot, *C. R. H. Acad. Sci. Ser. C* **265**, 183 (1967).
35. S. Andersson, J. Galy, and K. A. Wilhelmi, *Acta Chem. Scand.* **24**, 1473 (1970).
36. E. Gillis, *C. R. H. Acad. Sci.* **258**, 4765 (1964).
37. J. S. Anderson and B. G. Hyde, *J. Phys. Chem. Solids* **28**, 1393 (1967).
38. E. Gillis and G. Remaut, *C. R. H. Acad. Sci. Ser. B* **262**, 1215 (1966).
39. R. J. D. Tilley and B. G. Hyde, *J. Phys. Chem. Solids* **31**, 1613 (1970).
40. J. L. Ragle, *J. Chem. Phys.* **38**, 2020 (1963).
41. I. K. Krch, *Abh. Staats Univ. Saratov* **14**, 54 (1938).
42. A. I. Manakov, O. A. Esin, and B. M. Lepinskikh, *Dokl. Phys. Chem.* **142**, 171 (1962).
43. A. R. Tourky, Z. Hanafi, and K. Al Zervel, *Z. Phys. Chem. (Leipzig)* **242**, 218, 305 (1969).
44. L. Friedman and T. Holstein, *Ann. Phys.* **21**, 494 (1963).
45. J. B. Goodenough, *J. Solid State Chem.* **1**, 349 (1970).
46. T. C. Harman and J. M. Honig, "Thermoelectric and Thermomagnetic Effects and Applications," McGraw-Hill, New York, 1967.
47. E. Gillis and E. Boesman, *Phys. Status. Solidi* **14**, 337 (1966).
48. E. R. S. Winter, *J. Chem. Soc.* 2889 (1968).
49. V. S. Muzykantov, V. V. Popovskii,, G. K. Boreskov, and N. I. Mikickur, *Kinet. Catal. (USSR)* **5**, 665 (1964).
50. J. Nováková, K. Kliér, and P. Jiřů, *Reactiv. Solids, Int. Symp., 5th, 1964* (1965).
51. V. S. Muzykantov, P. Jiřů, K. Klier, and J. Nováková, *Collect. Czech. Chem. Commun.* **33**, 829 (1968).
52. For a general review of ^{18}O exchange on oxide catalysts see J. Nováková, *Catal. Rev.* **4**, 77 (1970).
53. N. A. Stukanovskaya and V. A. Roiter, *Kinet. Katal. Akad. Nauk. SSSR Sb. Statei* 216 (1960).
54. V. A. Roiter and V. A. Yuza, *Kinet. Catal.* **3**, 302 (1962).
55. J. H. Perlstein, Ph.D. Thesis, Cornell University (1967).